Materials Research Bulletin 44 (2009) 1528–1533

Contents lists available at ScienceDirect

Materials Research Bulletin

journal homepage: www.elsevier.com/locate/matresbu

Synthesis of TiC–TiB_2–Ni cermets by thermal explosion under pressure

D. Vallauri *, F.A. Deorsola

Politecnico di Torino, Dipartimento Scienza dei Materiali e Ingegneria Chimica, Corso Duca degli Abruzzi 24, 10129 Torino, Italy

ARTICLE INFO

Article history:
Received 9 December 2008
Received in revised form 2 February 2009
Accepted 12 February 2009
Available online 24 February 2009

Keywords:
A. Composites
B. Chemical synthesis
C. Electron microscopy
D. Microstructure

ABSTRACT

TiC/TiB_2-based cermets were fabricated in situ by means of the thermal explosion under pressure technique starting from Ti–B_4C powders with the addition of varying contents of Ni metal binder to achieve near-net-shape bulks. The combustion reaction was ignited in a graphite die heated by current. Full conversion of the reactants was obtained by thermal explosion and the process yielded TiC–TiB_2–Ni materials characterised by a fine microstructure. Appreciable differences in terms of microstructure, hardness and fracture toughness by indentation were observed between core and external surface of the products due to fast cooling caused by heat transfer to the die walls. Cermets with a high content of Ni showing high hardness and fracture toughness were obtained, with values of $HV_5 = 2182$ and $K_{Ic} = 8.8$ MPa $m^{1/2}$ for 30 wt.% Ni and of $HV_5 = 1684$ and $K_{Ic} = 12.7$ MPa $m^{1/2}$ for 47 wt.% Ni.

1. Introduction

Sintered carbides and borides, also referred to as refractory hardmetals, represent key materials in the modern industry for a number of demanding applications. Carbide–boride composites of transition metals are recognised as valid candidates for technological applications under extreme conditions due to their excellent combination of mechanical and electrical properties as well as their good corrosion and oxidation resistance at high temperatures [1]. For these properties, the use of TiC–TiB_2 in non-structural applications like wall tiles in nuclear fusion reactors, cathodes in Hall–Heroult cells and vapourising elements in vacuum–metal deposition installations have been under investigations [2,3]. Furthermore, in comparison to conventional cermets based on WC and TiC, cermets based on TiC–TiB_2 composites exhibit a higher hardness and chemical stability at high temperatures and are regarded as a good alternative for wear-resistant applications [4]. In this framework, TiC–TiB_2 composites represent promising materials for use as wear parts and cutting tools and also exhibit good behaviour as high-temperature structural components in heat exchangers and engines.

Due to the extremely high melting temperatures of TiB_2 and TiC, their high degree of covalent bonding and the low self-diffusion coefficients of the constituent elements, the processing of these ultra-refractory composites into components with full density through traditional routes requires extremely high temperatures. A number of new densification techniques have thus been investigated to overcome this problem, like for instance reactive sintering [5] or reactive hot pressing (RHP) [6], addition of "tailored" sintering aids in TiB_2–TiC composites [4], directional reaction of molten titanium with B_4C performs [7] and self-propagating high-temperature synthesis (SHS) assisted by a forced consolidation step [8]. Regarding cermets based on the TiC/TiB_2 system, composites with Ni addition were fabricated by a RHP process also referred to as displacement reaction under pressure [9,10]. On the other hand, researchers are continuously investigating solutions aimed at enhancing the specific tribological properties of metallic materials by fabricating metal matrix composites with ceramic reinforcements [11,12]. In this framework, nickel matrix composites were for instance developed through the use of SiC particulate additions [13], allowing an increase of hardness and the retention of values of fracture toughness compatible with the requirements of engineering applications.

SHS is based on highly exothermic reactions, which upon initiation, become self-propagating. Many ceramic materials including TiC and TiB_2 and their composites can be synthesized by means of SHS [14,15]. The SHS process allows the in situ synthesis of multi-phase materials, like in the case of TiC–TiB_2 composites. This important feature remarkably affects the product characteristics, since materials produced by SHS exhibit outstanding properties that are often better that those exhibited by the same composites produced by conventional routes (i.e. premixing of TiC and TiB_2 powders). However, the SHS products are porous and therefore have to be compacted and sintered to produce bulk components suitable for engineering applications [16]. An attractive alternative is the ability to apply pressure on the reaction products, thus leading to simultaneous synthesis and densification of the composite materials [17]. If the SHS process is

* Corresponding author. Tel.: +39 011 5644672; fax: +39 011 5644669.
E-mail address: dario.vallauri@polito.it (D. Vallauri).

0025-5408/$ – see front matter © 2009 Elsevier Ltd. All rights reserved.
doi:10.1016/j.materresbull.2009.02.009

conducted under the application of pressure, it is commonly referred to as high-pressure self-combustion synthesis (HPCS) which has been used in a number of studies [9,18,19] to consolidate TiC–TiB_2 composites. By following this approach, dense TiC–TiB_2–Ni composites have been fabricated by direct reaction of molten titanium with boron carbide preforms in the presence of a varying weight percentage of nickel [9,10] by pressure-assisted thermal explosion, which is a particular mode of conducting combustion synthesis reactions. The thermal explosion experiments were carried out in a rigid die preheated to 1000 or 1100 °C and subjected to a pressure of 150 MPa [20].

In this work, the simultaneous synthesis and densification of TiC–TiB_2–Ni cermets with Ni-rich compositions has been investigated by means of thermal explosion under pressure. The correlation between the synthesis process, the microstructure and the properties of the composites was investigated.

2. Experimental procedure

The reaction investigated for the fabrication of bulk TiC–TiB_2–Ni cermets was the following:

$$3Ti + B_4C + xNi \Rightarrow TiC + 2TiB_2 + xNi \quad (1)$$

Reactant powders of titanium (William Rowland, particle size −325 mesh, purity 99.3%), boron carbide (H.C. Starck, <10 μm, 99.8%) and nickel (Aldrich C.C. Fluka, 3 μm, 99.7%) were used in the experiments.

A nickel content x varying between 1.5 and 3 mol was used in the experiments. The theoretical compositions of the relative reaction products are shown in Table 1.

The reactant powders were mixed by ball milling for 12 h using stainless steel balls and vial and a ball-to-powder mass ratio equal to 5:1 and then dried in a furnace for 2 h at about 120 °C to remove adsorbed water. The dried powder mixture was then pressed in a steel die into pellets of 18 mm in diameter and 15–20 mm in height with a green density ranging between 55 and 65% TD.

The pressure-assisted thermal explosion (TE) experiments were carried out in a purposely designed and developed equipment, shown in Fig. 1. The green pellets were placed into the graphite mould. In order to avoid sticking of the samples to the walls of the die, the pellets were coated with a hexagonal BN spray acting as detaching and protective layer. A vessel filled with argon gas at atmospheric pressure was used in order to prevent damage of the graphite dies and punches due to the high temperature reached during the process. The heating of the green compacts was achieved by Joule effect through an electric current flowing through the graphite die and punches. The combustion synthesis reaction was therefore conducted in a thermal explosion mode, as the heating of the reactant mass is achieved simultaneously throughout the green compact. The heating of the reactant powders provides the formation of a Ni–Ti eutectic, with $T_m \cong 940$ °C [20], and the presence of liquid metal allows the reaction to take place at about 1000–1100 °C [21]. After the reaction was ignited, a pressure of 50–60 MPa was applied in order to densify the reacted material and to obtain bulk samples. The application of pressure was initiated after a certain delay time to allow the completion of the self-sustaining reaction. The overall pressure cycle is reported in Fig. 2. The delay time was optimised

Table 1
Theoretical composition of the products of the reaction $3Ti + B_4C + xNi$.

Products	x = 1.5 mol	x = 3 mol
TiB_2	48.4 wt.%	37.0 wt.%
TiC	20.9 wt.%	16.0 wt.%
Ni	30.7 wt.%	47.0 wt.%

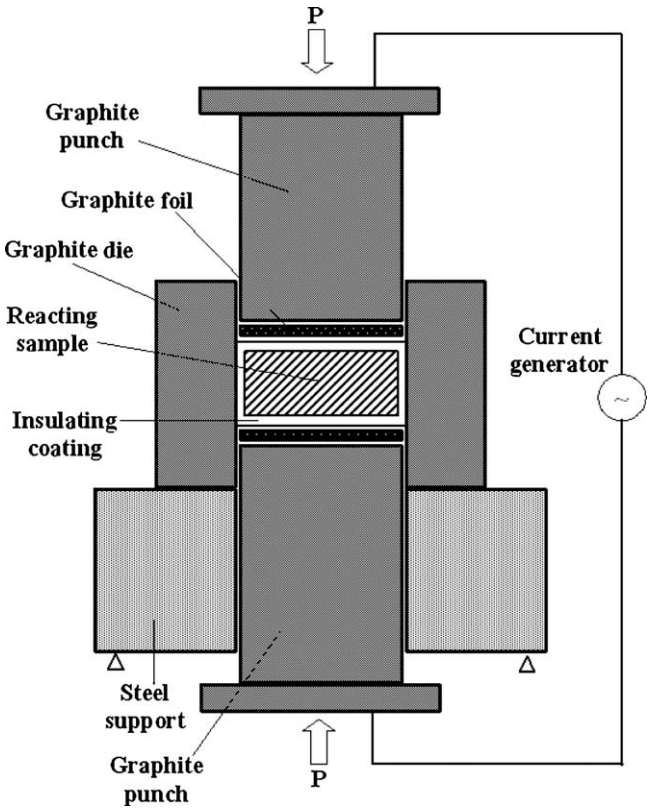

Fig. 1. Experimental setup for the fabrication of bulk TiC–TiB_2–Ni cermets by thermal explosion under pressure.

by measuring the values of the electrical characteristics (current and voltage) during the process by means of a high-speed multifunction acquisition board (National Instruments NI PCI-6251, 16 bit, range −10 to +10 V). The monitoring of the calculated electrical resistance with a sampling frequency of 1.25 ms/s allowed a very accurate process control and the identification of the optimum delay time for the pressure application, as discussed in the following section.

The reaction products in the bulk materials obtained by thermal explosion under pressure were identified by X-ray diffraction by an X'Pert Philips diffractometer with a Cu Kα radiation (λ = 0.154060–0.154439 nm) and a count time of 1 s per 0.02° step. The density of the compacts was measured by the volume displacement method. Microstructural observations were carried out on polished surfaces in a LEO SUPRA 40 Field-emission

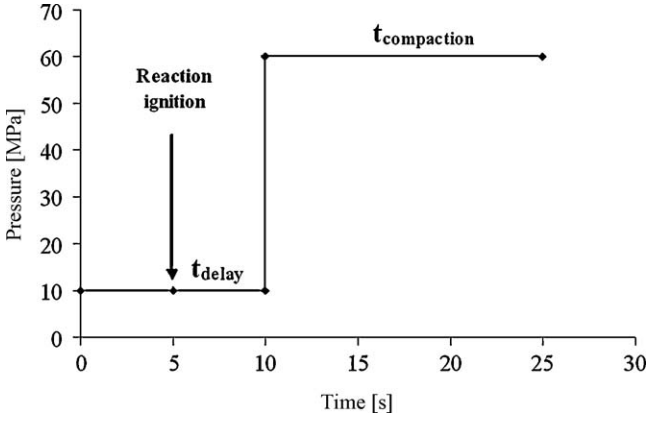

Fig. 2. Pressure cycle used in the pressure-assisted TE tests of TiC–TiB_2–Ni cermets.

scanning electron microscope (FESEM) equipped with back scattering electron (BSE) imaging and EDAX microprobe. The Vickers microhardness and hardness were measured at loads of 4.9 and 98.1 N using a Leitz Wetzlar 8585 and an Amsler Wolpert Dia Testor 2RC diamond indenters, respectively. Therefore the values of Vickers hardness $HV_{0.5}$ and HV_5 were determined. The cracks that originated from the Vickers indentations were also used to compute the fracture toughness by the IF method, according to the following equation derived from Palmqvist [22]:

$$K_{Ic} = 0.0319\left(\frac{P}{al^{1/2}}\right) \quad (2)$$

where P is the indentation load (N), a is the indentation half-diagonal length (m) and l is the surface radial crack length (m). For all the loads, the ratio l/a between the crack length and the indentation half-diagonal was within the empirical limits of Palmqvist cracks, i.e. $0.25 \leq l/a \leq 2.5$. In order to evaluate the influence of the microstructure on hardness and fracture toughness, two series of indentations were carried out, in the centre and on the peripheral border (300 μm from the external surface) of the sample, respectively. The values of hardness and fracture toughness reported in this paper are an average of six measurements.

3. Results and discussion

The possibility of acquisition of the current/voltage values turned out to be very useful for a reliable process control, allowing the calculation of the electrical resistance of the reacting sample in a continuous way during the overall heating process. The resistance of the sample was then selected as the key parameter for the determination of the reaction ignition time reported in Fig. 2. A very intense peak was recorded at the time of ignition of the thermal explosion reaction, as shown in Fig. 3. During the heating step, the electrical resistivity of the reactant mixture increases by increasing the temperature. Once the reaction starts, the temperature rises very fast and consequently also the resistivity is increased. The resistivity is also increased due to the formation of the ceramic phases after the reaction. Therefore the intense peak highlighted in Fig. 3 corresponds to the reaction ignition time. In this way, the exact time for pressure application was accurately determined after a delay time of 5 s, and pressure was applied to compact the reaction products while they were in a plastic state favoured by the formation of molten nickel.

The TE reaction is completed after a few seconds from the ignition. As can be drawn from Fig. 3, the heating of the reactant mixture was very fast and the ignition of the reaction took place after 3 s. The compaction was applied after 10 s from the beginning. The overall cycle of TE under pressure was completed in about 25 s. This very short cycle and the very fast heating can be very beneficial for the synthesized material, as long times at high temperature can induce a considerable coarsening of the microstructure.

Fig. 4 shows the XRD pattern for the products obtained by reaction (1) with a content of 1.5 mol Ni. Pure TiC, TiB_2 and Ni products were detected with no peaks indicative of unreacted Ti and B_4C or undesired intermetallic phases of the Ni–Ti system and Ti_3B_4 or TiB transient compounds, thus indicating that full conversion of reagents into products was achieved according to reaction (1). It has also to be remarked that no evidence of formation of undesired reaction products, like, e.g. Ni_xB_y was found. These phases are commonly formed when processing TiC–TiB_2 or TiB_2-based cermets with a high content of Ni by traditional consolidation techniques [10,23], and cause a detrimental embrittlement of the composites [24]. However, the very short processing times required by the pressure-assisted TE under investigation hindered the occurrence of diffusion-driven interface reactions and did not allow the formation of these undesired phases. This observation was confirmed by the good properties measured on the developed composites, as will be discussed below.

The representative microstructure of the samples obtained by TE under pressure with 1.5 mol Ni is shown in Fig. 5. As previously mentioned, the basic principle of the process deals with the formation of a liquid phase due to the melting of the Ni–Ti eutectic occurring by heating the reactant powder blend into the graphite die. This liquid phase favours the ignition of the reaction between Ti and B_4C and the production of the TiC and TiB_2 phases. A proper pressure application in the presence of the liquid phase permits thus to obtain a high-density bulk part. The final result of the process is the formation in situ of a cermet consisting of a TiC–TiB_2 ceramic phase surrounded by a Ni matrix, which is represented by the light grey phase observed in Fig. 5.

The microstructural characterisation revealed a significant difference between the core and the periphery of the samples. The difference is evident in Fig. 5, as the microstructure appears appreciably finer at the periphery with respect to the inner core of the sample. This is probably due to the fact that the cooling rate in the outer zone is higher due to the contact with the wall of the die. This fact produces a grain refinement, leading to the formation of crystalline grains of the ceramic phases with average size smaller than 1 μm and the inhibition of their growth due to the more rapid cooling. This is in good agreement with the results of modelling activity reported in the literature [25], showing an enhanced cooling rate of the surface due to the contact with the pressing die. Moreover, also the Ni content appears to be lower in the peripheral

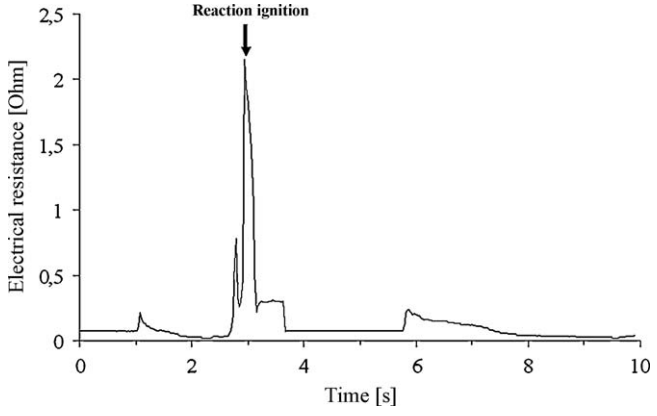

Fig. 3. Electrical resistance vs. cycle time plot recorded during the TE under pressure process.

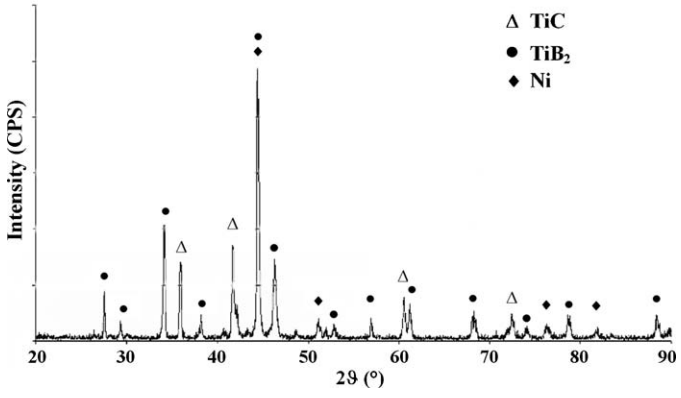

Fig. 4. XRD pattern of the TiC–TiB_2–1.5 mol Ni cermets obtained by pressure-assisted TE.

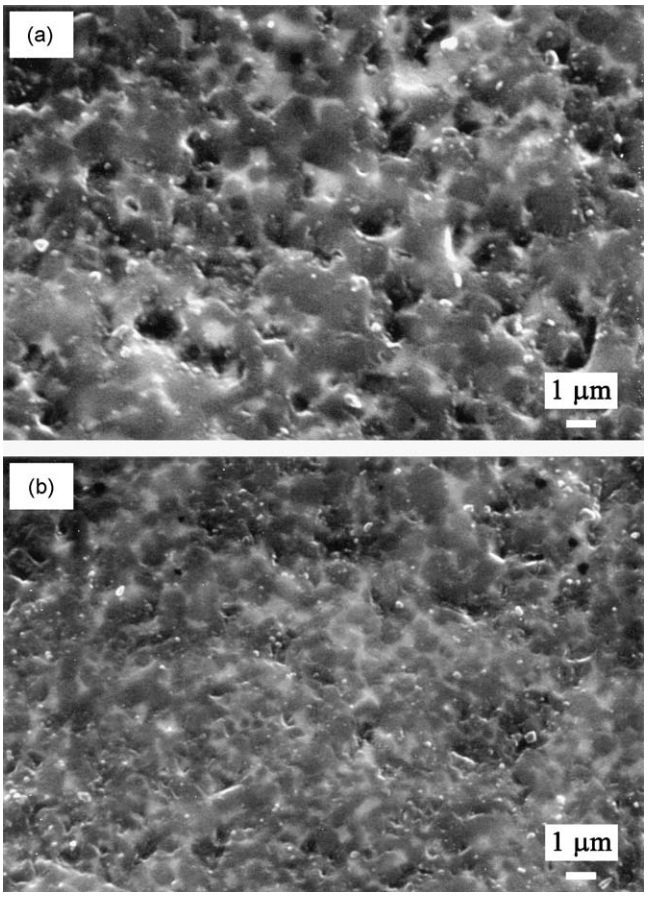

Fig. 5. (a) and (b) SEM micrographs showing the microstructure of bulk TiC–TiB_2–1.5 mol Ni cermets consolidated through pressure-assisted thermal explosion: centre (a) and peripheral border (b) of the sample.

section of the sample, as demonstrated by the SEM observations. This fact can be explained with a possible loss of metal binder that is squeezed out of the surface due to the compaction pressure. In agreement with this, small amount of metal were observed on the wall of the die after recovering the samples at the end of the process.

By SEM observations, the shape of the ceramic TiC and TiB_2 grains appears squared in the case of the cubic TiC phase and elongated platelet-like in the case of the hexagonal TiB_2 phase. This is due to the fact that the content of metal phase and the very short processing time did not allow the occurrence of the typical mechanisms of solution of the ceramic phase into the liquid metal, and its subsequent re-precipitation. The carbide/boride grains can be partially dissolved into the binder phase and then re-precipitate. As the sharp edges of the ceramic grains are more like to be brought into solution, these phenomena produce a ceramic phase characterised by rounded shape. These phenomena noticeably affect the size and shape of the grains, the interface with the binder, and, as a result, the properties of the obtained material. Regarding the dissolution, when the grains of TiC and TiB_2 are fine, their solubility would be higher in the molten Ni binder during the process. For this reason the shape of the ceramic grains in the samples containing 1.5 mol Ni appear more rounded in the periphery of the cermet. On the other hand, ceramic grains with sharp edges were observed in the microstructure of the centre of the sample, with the two phases easily distinguishable as shown in Fig. 6.

Similar observations were drawn increasing the Ni content into the starting mixture. As a comparison, the microstructure of a

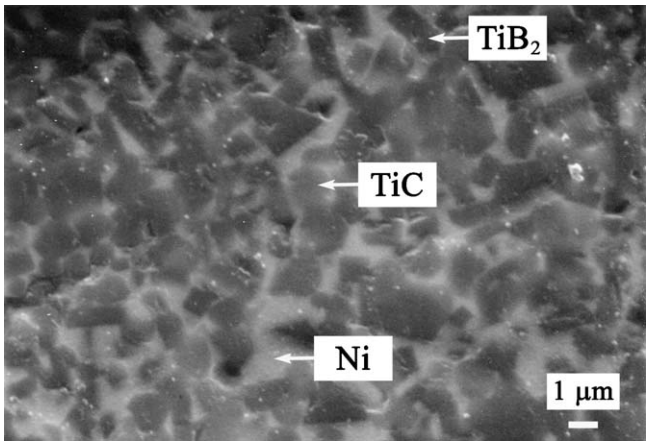

Fig. 6. SEM micrographs showing the microstructure in the centre of bulk TiC–TiB_2–1.5 mol Ni cermets consolidated through pressure-assisted thermal explosion. The microstructure consisted of equiaxed TiC grains and elongated TiB_2 grains in a metallic Ni matrix.

sample with a nickel content of 3 mol is shown in Fig. 7. Also in this case the reacted samples show a homogeneous and fine-grained microstructure, with grain size ranging between 1 and 5 μm. Anyway, the rounded shape of the ceramic TiC and TiB_2 grains points out that the higher content of metal phase is responsible for solution/re-precipitation phenomena occurring during the TE under pressure process as demonstrated by the SEM observations, less evident in the samples containing a lower content of Ni. This behaviour was particularly evident in the samples containing

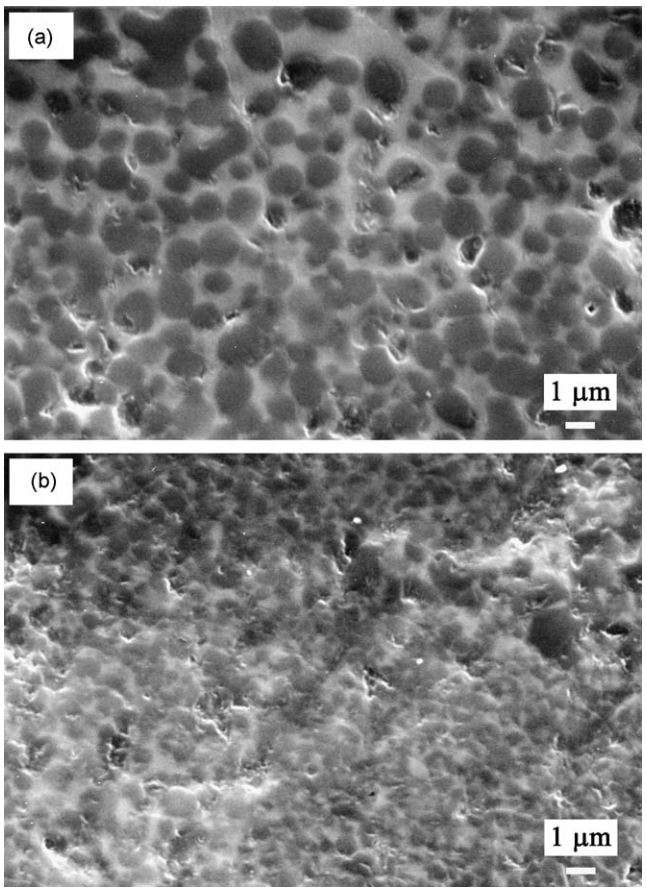

Fig. 7. (a) and (b) SEM micrographs showing the microstructure of bulk TiC–TiB_2–3 mol Ni cermets consolidated through pressure-assisted thermal explosion: centre (a) and peripheral border (b) of the sample.

Table 2
Properties measured on the bulk TiC–TiB_2–Ni cermets fabricated through TE under pressure from 3Ti + B_4C + xNi mixtures.

Ni content (mol)	Theoretical composition (wt.%)	Density (g/cm^3)	Zone of the samples	Vickers hardness and standard deviation (σ)		Fracture toughness K_{Ic} (MPa m$^{1/2}$) and standard deviation (σ)
				$HV_{0.5}$	HV_5	
1.5 Ni	TiB_2; 20.9 TiC; 30.7 Ni	5.17	Core	2252 (269)	1647 (308)	6.7 (0.9)
			Border	2880 (312)	2182 (381)	8.8 (1.4)
3 Ni	TiB_2; 16.0 TiC; 47.0 Ni	5.86	Core	1873 (195)	1587 (65)	11.6 (1.7)
			Border	2081 (202)	1684 (156)	12.7 (1.9)

3 mol Ni binder. In fact, both the ceramic phases have a limited solubility in molten Ni (11 wt.% at 1400 °C for TiC [26] and 0.5 mol% at the eutectic temperature for TiB_2 [27]). Therefore the solution/re-precipitation mechanisms were significantly enhanced by increasing the Ni content in the starting mixture. The behaviour was particularly evident in the centre of the cermets containing 3 mol of Ni (Fig. 7a), where the content of melted Ni appeared higher.

A behaviour correlated with the microstructural characteristics was observed in terms of mechanical properties of the materials, which exhibited significant differences between the core and the periphery of the samples. The values of Vickers microhardness, hardness and fracture toughness by indentation measured at the centre and at the periphery are summarised in Table 2. Regarding the density of the cermets, the determination of the theoretical density was not possible due to the loss of a certain fraction of molten Ni possibly squeezed out of the samples during the process due to the compaction pressure. However, the microstructural observations demonstrated that nearly full density was achieved in the case of the cermets containing 3 mol Ni, whereas a certain degree of residual porosity was found in the cermet with a lower content of metal binder.

As can be seen, the measured properties were in good agreement with the previously discussed microstructural observations. In fact, the hardness values measured in the periphery of the samples resulted significantly higher than those measured in the centre, for both the cermets containing 1.5 and 3 mol Ni. This was due to the finer microstructure observed in the periphery of both samples. The higher hardness measured at the periphery of the samples was due to a combination of refined microstructure and lower content of Ni observed in that area of the samples. The calculated standard deviation resulted higher in the periphery of the samples. This was probably due to a much regular and homogeneous microstructure shown in the core of the cermets. Regarding the content of metal binder, a higher standard deviation was calculated for the cermets with 1.5 mol Ni, due to the larger amount of residual porosity observed in these composites. However, the cermets showed very high values of hardness considering the high contents of metal binder, in particular for the composite containing 3 mol Ni (corresponding to 47 wt.% of metal phase).

A similar behaviour was observed for the fracture toughness by indentation, that resulted lower in the centre of the samples than at the periphery for both the cermets containing 1.5 and 3 mol Ni. The higher fracture toughness measured at the periphery can be explained as the result of the very fine microstructure formed on the outer surface. As a general assumption, the fracture toughness in cermets decreases with decreasing the grain size of the hard phases. However, the higher fracture toughness measured in the areas of the present composites showing a finer microstructure is in good agreement with the results obtained by Chenhui et al. [28] for Ti(C,N) cermets. The authors report that for those composites the fracture toughness increased with the decrease of the grain size of the hard phases. This observation seems to be valid in particular for metal ceramic composites characterised by the absence of the core/shell structure typical of the cermets, i.e. the presence of coreless grains can be regarded as beneficial for the toughness of the cermets [29]. In this condition, the refinement of the microstructure induces a significant improvement of the toughness, like observed for ultrafine (Ti,W)C–Ni cermets [30]. The TiC–TiB_2–Ni cermets developed in this work correspond to this condition, as no evidence of formation of a core/rim structure was found in the ceramic grains. The explanation for the difference observed in the indentation toughness in the different sample zones is probably correlated with the crack propagation mechanisms. It is reported that crack propagation in cermets generally occurs by transcrystalline fracture of the hard phase grains in coarse-grained materials, whereas intercrystalline or intergranular rupture is predominant in fine-grained cermets. Thereby, the crack propagation path is longer in cermets with fine-grained microstructures [31]. This observation gives a possible explanation for the higher indentation toughness measured in the fine-grained periphery of the samples fabricated by TE under pressure, despite of the lower content of Ni observed in those areas. In addition to this, a stronger interface between hard phases and binder possibly present in the periphery of the cermets due to higher solubility of the fine grains can contribute to the toughening of the microstructure by increasing the intercrystalline rupture strength in the surface of the samples.

The comparison reported in Table 3 demonstrates that the properties of the developed materials favourably compare with those reported in selected literature works for similar cermets in terms of hardness and fracture toughness. In particular, the TiC–TiB_2–Ni cermets developed in this work showed on the outer surface higher values of microhardness and of fracture toughness than those reported for cermets with similar composition. This behaviour can be explained with the fine-grained microstructure observed in the TiC–TiB_2–Ni cermets developed in this work.

Table 3
Comparison between the properties measured on the bulk TiC–TiB_2–Ni cermets fabricated by TE under pressure and similar materials found in selected literature works.

Metal binder content (wt.%)	Material composition	Density (absolute or relative)	Processing route	Vickers hardness HV_x	Fracture toughness K_{Ic} (MPa m$^{1/2}$)	Reference
30.7 wt.% Ni	TiB_2–TiC–Ni	5.17 g/cm^3	TE under pressure (60 MPa)	2880 ($HV_{0.5}$), 2182 (HV_5)	8.8	This work
47.0 wt.% Ni	TiB_2–TiC–Ni	5.86 g/cm^3	TE under pressure (60 MPa)	2081 ($HV_{0.5}$), 1684 (HV_5)	12.7	This work
30.7 wt.% Ni	TiB_2–TiC–Ni	~99% TD	TE under pressure (150 MPa)	2528 ($HV_{0.5}$), 1620 (HV_{20})	6.8	[9]
30.7 wt.% Ni	TiB_2–TiC–Ni	~99% TD	Reactive hot pressing (150 MPa)	2619 ($HV_{0.5}$), 1794 (HV_{20})	6.8	[9]

Considering the simplicity of the compositions and the exhibited properties, the developed TiC–TiB_2–Ni cermets show great potential for wear-resistant applications. In this view, the improved hardness and fracture toughness exhibited on the external surface may be beneficial as the best properties are shown on the working areas of the material.

4. Conclusions

TiC–TiB_2 cermets with a high content of Ni binder (30.7 and 47 wt.%) were successfully fabricated through the thermal explosion under pressure process. In both compositions, a significant refinement of the grain size of the ceramic phases was observed on the external surface of the cermets, due to heat transfer between reacted material and graphite die. This phenomenon, combined with a lower content of Ni observed on the periphery due to the compaction pressure, led to a remarkable increase of the surface hardness. A higher fracture toughness was also measured on the periphery of the samples, possibly due to a predominant intercrystalline rupture mechanism and an enhanced interface bonding between Ni binder and fine-grained ceramic phases. The developed Ni-rich cermets with enhanced surface properties are potentially very interesting for wear-resistant applications.

Acknowledgement

This work is part of the project INCOSYNT, supported by the European Commission under the contract G1ST-CT-2000-50011.

References

[1] D. Vallauri, I.C. Atías Adrián, A. Chrysanthou, J. Eur. Ceram. Soc. 28 (8) (2008) 1697–1713.
[2] X. Zhou, S. Zhang, M. Zhu, B. Chen, Int. J. Self-Prop. High-Temp. Synth. 7 (1998) 403–408.
[3] D. Brodkin, S. Kalidindi, M. Barsoum, A. Zavaliangos, J. Am. Ceram. Soc. 79 (7) (1996) 1945–1952.
[4] T.J. Davies, A.A. Ogwu, Powder Metall. 38 (1) (1995) 39–44.
[5] H. Zhao, Y.-B. Cheng, Ceram. Int. 25 (1999) 353–358.
[6] G. Wen, S.B. Li, B.S. Zhang, Z.X. Guo, Acta Mater. 49 (2001) 1463–1470.
[7] S.K. Lee, D. Kim, C.K. Kim, J. Mater. Sci. 29 (1994) 4125–4130.
[8] R. Tomoshige, Y. Kakoki, K. Imamura, A. Chiba, J. Mater. Process. Technol. 85 (1999) 105–108.
[9] I. Gotman, N.A. Travitzky, E.Y. Gutmanas, Mater. Sci. Eng. A 244 (1998) 127–137.
[10] E.Y. Gutmanas, I. Gotman, Ceram. Int. 26 (2000) 699–707.
[11] S.C. Tjong, Z.Y. Ma, Mater. Sci. Eng. R 29 (2000) 49–113.
[12] Y.-F. Yang, H.-Y. Wang, Y.-H. Liang, R.-Y. Zhao, Q.-C. Jiang, Mater. Sci. Eng. A 445–446 (2007) 398–404.
[13] M. Srivastava, V.K.W. Grips, A. Jain, K.S. Rajam, Surf. Coat. Technol. 202 (2007) 310–318.
[14] C.L. Yeh, Y.L. Chen, J. Alloy Compd. 463 (2008) 373–377.
[15] B. Zou, P. Shen, Z. Gao, Q. Jiang, J. Eur. Ceram. Soc. 28 (2008) 2275–2279.
[16] A. Chrysanthou, Y.K. Chen, A. Vijayan, J.M. O'Sullivan, J. Mater. Sci. 38 (2003) 2073–2077.
[17] Z.A. Munir, U. Anselmi-Tamburini, Self propagating high temperature synthesis of hard materials, in: R. Riedel (Ed.), Handbook of Ceramic Hard Materials., Wiley-VCH, New York, 2003, pp. 322–338.
[18] Z.Y. Fu, H. Wang, W.M. Wang, R.Z. Yuan, J. Mater. Process. Technol. 137 (2003) 30–34.
[19] Z. Xinghong, Z. Chungcheng, Q. Wei, V.L. Kvanin, Compos. Sci. Technol. 62 (2002) 2037–2041.
[20] E.Y. Gutmanas, I. Gotman, J. Eur. Ceram. Soc. 19 (1999) 2381–2393.
[21] S.K. Bhaumik, C. Divakar, A.K. Singh, G.S. Upadhyaya, Mater. Sci. Eng. A 279 (2000) 275–281.
[22] D.K. Shetty, I.G. Wright, P.N. Mincer, H. Clauser, J. Mater. Sci. 20 (1985) 1873–1882.
[23] W.-J. Kim, D.-H. Kim, E.S. Kang, D.K. Kim, C.H. Kim, J. Mater. Sci. 31 (1995) 5805–5809.
[24] K.B. Shim, M.J. Edirisinghe, B. Ralph, Br. Ceram. Trans. 95 (1) (1996) 15–22.
[25] M. Shapiro, I. Gotman, V. Dudko, J. Eur. Ceram. Soc. 19 (1999) 2233–2239.
[26] P. Ettmayer, H. Kolaska, W. Lengauer, K. Dreyer, Int. J. Refract. Met. H 13 (1995) 343.
[27] J.M. Sanchez, M.G. Barandika, J. Gil-Sevillano, F. Castro, Scripta Metall. Mater. 26 (1992) 957–962.
[28] L. Chenhui, Y. Lixin, X. Weihao, Acta Mater. Compos. Sinica 20 (1) (2003) 1–6.
[29] X. Zhang, N. Liu, C. Rong, J. Zhou, Ceram. Int. 35 (2009) 1187–1193.
[30] S. Park, S. Kang, Scripta Mater. 52 (2005) 129–133.
[31] N. Liu, W. Yin, L. Zhu, Mater. Sci. Eng. A 445–446 (2007) 707–716.